Current Research in Biotechnology 2 (2020) 64–73

Contents lists available at ScienceDirect

Current Research in Biotechnology

journal homepage: www.elsevier.com/locate/crbiot

Unusual microbial community and impact of iron and sulfate on microbial fuel cell ecology and performance

Lucca Bonjy Kikuti Mancílio [a,b], Guilherme Augusto Ribeiro [a], Erica Mendes Lopes [b], Luciano Takeshi Kishi [c], Leonardo Martins-Santana [d], Guilherme Marcelino Viana de Siqueira [d], Adalgisa Rodrigues Andrade [a], María-Eugenia Guazzaroni [b], Valeria Reginatto [a,*]

[a] Department of Chemistry, Faculty of Philosophy Sciences and Letters of Ribeirão Preto - FFCLRP, University of São Paulo, Av. Bandeirantes 3900, CEP 14040-030, Ribeirão, Preto, SP, Brazil
[b] Department of Biology, FFCLRP, University of São Paulo, Ribeirão Preto, Brazil
[c] National Laboratory of Scientific Computing, Petrópolis, Brazil
[d] Department of Biochemistry and Immunology, FMRP - University of São Paulo, Ribeirão Preto, Brazil

ARTICLE INFO

Article history:
Received 15 December 2019
Received in revised form 25 March 2020
Accepted 3 April 2020

Keywords:
Electroactive marine sediment
Core community
Bioelectricity
Bioremediation

ABSTRACT

The present energy and the waste accumulation crisis make the development of bioelectrochemical systems each day more important as a technology for coupled waste-treatment, electricity production, and biorefinement, whilst closing the circular economy loop. However, its application is still hampered by the complexity of its biocatalysts. This study evaluated, from an ecological and metabolic point of view, Microbial Fuel Cells (MFCs) inoculated with Brazilian marine sediment and fed with synthetic wastewaters contaminated with iron and sulfate, containing acetate as carbon source. Making use of 16S rRNA gene amplification analyses and physical- and electrochemical assays, a stable core community was observed throughout different treatments, lacking in the taxa traditionally affiliated with MFCs, while rich in alkaliphiles and acetogens, namely *Desulfomicrobium, Advenella, Tindallia, Clostridium,* and *Desulfuromonas*. MFCs supplemented with iron and sulfate obtained more stable electrochemical performances, although the core microbial community remains unchanged, apart from a slight shift within the relative dominance of each group within the core. The use of these common pollutants affected the nutritional profile by activating different metabolic pathways for iron and sulfate cycling coupled to the ubiquitous nutrients, while strongly influencing ammonia balance. This study highlights the hidden potential to be explored in novel inocula from this still poorly investigated Southern Hemisphere and provides insights into what may be used as tools to better manipulate the communities constituting MFC bioanodes.

1. Introduction

The heavy reliance on fossil resources as well as their polluting potential has driven the search for alternative sources and technologies towards a cleaner and more sustainable power generation (Mohan et al., 2014). Meanwhile, the exacerbated generation of heavily polluting byproducts by a variety of industries poses a threat to the environment and has become a topic of both public health and safety discussion (Mohan et al., 2014).

Bioelectrochemical systems emerge as an opportunity to link the resolution of both the dwindling supply of fossil fuels and the ever-increasing need for better waste and pollutant management technologies. MFCs are such systems that use microbial cultures to produce electricity (Logan, 2008). Through the use of microbial bioelectrocatalysis, MFCs can convert chemical energy released during metabolic processes into electric energy by compartmentalizing oxidoreductive reactions which otherwise would consume the electrons made available by these reactions in the ecological webs (Logan and Regan, 2006).

Although approaches to associate waste treatment and bioenergy production have long been known, such as biogas production, MFCs present a variety of advantages given the direct conversion of organic matter into electricity: they do not require gas treatment since the only gas produced is carbon dioxide, which has no useful energy content; and finally, they result in almost no solids/sludge production (Vilas Boas et al., 2019).

After over a decade of intense study of MFC electrode materials; pure bacterial strains as biocatalysts; and reactor configuration (Janicek et al., 2014; Watson and Logan, 2010; Yang et al., 2015; Yong et al., 2011), microbial biofilm formation on anode remains the most direct and key element to affect energy generation (Venkata Mohan et al., 2008). There is a wide spectrum of factors - that may affect biofilm formation and composition. However, most general knowledge about this field is currently based on *Geobacter* or *Shewanella* genera and acetate or lactate as electron donor (Liu et al., 2017), which limit such studies given that these models are predominantly heterotrophs, whereas natural microbial communities contain a myriad lithotrophs, even associated with nutrient cycling of compounds

* Corresponding author.
E-mail address: valeriars@ffclrp.usp.br. (V. Reginatto).

http://dx.doi.org/10.1016/j.crbiot.2020.04.001

hardly disposed by anthropic waste streams, such as metals. Thus, the study of ecological effects of such compounds on energy metabolism may clarify application strategies to treat such waste containing compounds and facilitate electron donation more independent from organic carbon supply. Furthermore, by understanding the complex web of processes happening within MFCs makes it possible not only to identify pure cultures equivalent to *Geobacter* and *Shewanella*. The development of this knowledge can open doors to bridge the metabolic complexity of mixed cultures and a metabolic restriction of pure cultures. The creation of artificial communities, with microbial components specifically selected or engineered for each situation, may be the middle ground needed for this leap in approach and application. Electricity generation thresholds in individual MFCs haven't evolved much in over a decade because of the natural limits of the acetate oxidation potential and diffusion capacity of cathodes, although it is possible to overcome these voltages with miniaturization, modularity and stacking of MFCs (Gajda et al., 2018). But controlling the oxidation processes occurring inside the MFCs in order to generate not only energy, but also added value products, remains a relatively unexplored opportunity, achievable through the minute understanding of ecological relationships within communities and how they are affected by the compounds in each scenario.

Of such potential compounds, attention has been drawn to iron and sulfur, which are regularly found in a variety of waste streams such as detergent manufacture, textile, paper and pulp, bleach and photographic industries, acid mine drainage, and mineral processing wastewater (Miran et al., 2017), being the study of the individual effects of each component ion different ratios considered essential for better engineering specifically directed approaches (Miran et al., 2017).

These ions can impact bioelectrochemical systems both biotically or abiotically. Biotically, the intrinsical participation of ions as cofactors can influence special protein levels and activity, possibly affecting energy metabolism and unlocking distinct metabolic pathways (Cvetkovic et al., 2010; Ruiz-Urigüen et al., 2018a). Otherwise, in the abiotic pathway, the metallic ions are responsible for electron shuttling, redox reactions, catalysis or precipitations (Lu et al., 2015).

Iron's role has already sparked investigation interest in bioelectrochemical systems, mainly in its ferrous form and through synthetic salts. For example, ferric iron, such as ferric- nitrilotriacetate NTA is commonly used as an inorganic electron acceptor for agar-based isolation of exoelectrogenic bacteria. Ferric iron has also been shown to affect *Pseudomonas* biofilm formation (Kisch et al., 2014). However, the impact of iron in its more readily available forms such as the one found in waste streams (naturally occurring rust) on mixed culture ecology and energy metabolism still remains obscure. As a consequence, the response of the exoelectrogenic community in the electrode biofilms to ferric iron is less investigated (Wei et al., 2013).

Sulfur is also a very interesting target for MFC investigation, due not only to its large presence in waste streams but also to its role in metal-precipitation (Alexandrino et al., 2014a) and the important contribution played by sulfur-reducers in MFC communities, especially *Desulfuromonas* and *Desulfovibrio (*Kumar et al., 2017a*)*. MFC technology has been suitably evaluated as an improvement strategy to biosulfidogenic metal removal (Miran et al., 2017). Sulfate can easily be converted to sulfide, which can act as an electron shuttle, which can be oxidized to elemental sulfur, and can be reduced again to sulfide, along with anodic back-oxidation of the elemental sulfur to sulfate (Daghio et al., 2018; Kumar et al., 2017a; Matturro et al., 2017).

Despite the diversity of available studies concerning iron and sulfate in MFCs, most of them focus on the abiotic effect of the addition of these metals or rather do not directly evaluate their effect over both microbial community composition and energy metabolism. In this study, electrochemical performances of MFCs supplemented with naturally found iron oxide and sulfate were investigated to reveal the response of the microbial community on the electrode biofilm to semi-ubiquitous forms of these compounds. Microbial community of the anode in MFCs were analyzed using metataxonomic analysis and related to the monitoring of nutritional availability.

2. Materials and methods

2.1. Microbial fuel cell construction and operation

An H-conformation cell was constructed where both compartments contained 250 mL, 200 mL of which were filled with culture media in the anode, and water in the cathode. The cathode made of 20% Pt (A6 ELAT®) was heat pressured with a NAFION® NRE-212 membrane as described before (Dos Passos et al., 2019) and this compartment was filled with distilled water. This proton-exchange membrane allows proton flux to keep pH balanced without gas intrusion or contamination. The anode consisted of a 6 cm^2 carbon cloth (BASF) spaced at 5 cm from the cathode, and immersed in anaerobic anodic culture media (sparged with N_2 gas), inoculated with marine sediment collected from the port of Rio Grande, in southern Brazil (coordinates 32°07′S 52°05′W) (Perazzoli et al., 2018). Three different fuels were supplied to the MFCs, acetate (MFC_A); acetate plus iron (MFC_Fe), and acetate plus sulfate (MFC_S), corresponding to those described by (Lovley and Phillips, 1988); (Lovley, 1993). The MFC_A medium was composed by: sodium acetate: 1 g/L; $NaHCO_3$: 2.5 g/L; Na_2HPO_4: 0.74 g/L; $Na_2HPO_4.H_2O$: 0.6 g/L; NH_4CL: 1;5 g/L; $MgCL_2•6H_2O$: 0.1 g/L; $MgSO_4.7H_2O$: 0.1 g/L; Yeast Extract: 0.05 g/L; $CaCl_2.2H_2O$: 0.1 g/L; KCl: 0.1 g/L; NaCl: 0.1 g/L; $NaMoO_4.2H_2O$: 0.001 g/L; $MnCl_2.4H_2O$: 0.005 g/L; while the MFC_Fe medium was identical to MFC_A medium with the addition of 100 mM (15.9 g/L) of Fe_2O_3. The MFC_S medium consisted of sodium acetate: 1 g/L; Na_2SO_4: 9 g/L; KH_2PO_4: 0.5 g/L; $MgCl_2.6H_2O$: 0.1 g/L; $CaCl_2.6H_2O$: 0.041 g/L; $MgSO_4.7H_2O$: 0.123 g/L; yeast extract: 1 g/L; sodium citrate: 0.342 g/L; $FeSO_4.7H_2O$: 0.1 g/L; $Na_2S.7H_2O$ 0.4%: 5 mL/L. The anaerobiosis was induced through N_2 gas sparging and confirmed by the addition of 1 mL/L resazurin (at 1% *w/v*) in each medium, whose lack of color indicated anaerobiosis. The first 7 days were dedicated to anodic biofilm growth, after this period the inoculating-sediment was removed under N_2 and the MFCs were fed with their respective medium. The feeding procedure was repeated every time the potential dropped near to zero, at these moments two and ten milliliters of samples were also collected for HPLC and spectrophotometric analysis, respectively.

2.2. Chemical analyses

Samples of the culture media were collected every cycle the MFCs were fed (ca. every 7 days), along with the fresh medium, for comparison. Acetate concentrations were monitored with high-performance-liquid-chromatography with Aminex HPX-87H column (7.8 mm × 300 mm) at 60 °C under isocratic conditions and 0.005 mol/L H_2SO_4 mobile phase at a flow rate of 0.6 mL/min (60 kgf / cm^2). A Refractive Index Detector (RID) coupled to LabSolutions software was used and Ionic-Chromatography (Methrom Pensalab Compact 881) with conductivity detector and METROSEP A SUPP 5, with eluent solution 3.1 $mmol.L^{-1}$ Na_2CO_3 and 1 $mmol.L^{-1}$ $NaHCO_3$ was used for sulfate, nitrate, and nitrite. Ion suppression in anion determination was performed using H_2SO4 (J.T. Baker) to decrease background conductivity (dos Reis, 2016).

Ammoniacal nitrogen was determined using the colorimetric Nessler protocol (Vogel, 1980).

Iron in its Fe^{2+} and Fe^{3+} forms was determined by the 1–10 phenanthroline colorimetric method by reaction with hydroxylamine chloride and absorbance reading at 510 nm (Clesceri and American Public Health Association, 2005).

To detect CO_2, CH_4, and H_2, in the headspace of the bioanodes, a gas sample was collected with a gas-tight syringe and analyzed in a Gas Chromatograph (CG 2014, Shimadzu, Japan). The analyses were performed in a CG, equipped with a thermal conductivity detector (DCT) and molecular sieve 5A (2.0mx 4.7 mm), with argon carrier gas at 30 mL/min flow rate.

2.3. Electrochemical measurements

The MFCs were operated at constant resistance mode connecting a 1000 Ω resistor at the external circuit, which is the most commonly used in literature for lab-scale reactors (Mei et al., 2015; Ruiz-Urigüen et al., 2018b; Sangcharoen et al., 2015; Sharma et al., 2016). The acquisition voltage of the cell was monitored continuously by an Arduino® Uno system. After MFC stabilization for at least 5 days cyclic voltammetric (CV) and polarization curves were performed at a Solartron 1480 potentiostat/galvanostat. First, the polarization curves of the MFC were obtained scanning (1 mV/s) between the respective open-circuit voltage (OCV) to zero for each system using the bioanode as counter-electrode, and cathode as both work- and reference-electrode. The OCV obtained ranged around 70 mV with the medium of MFC (MFC_A = 776 mV; MFC_Fe = 783 mV; MFC_S = 705 mV). To monitor the CV of the bioanode a conventional three-electrode system was prepared. Using the bioanode as work electrode, a platinum counter-electrode and a saturated calomel electrode (SCE) as reference. The CV mas registered at a low scan rate (1 mV/s) from −0.6 to +0.6 V vs SCE.

2.4. DNA extraction and Illumina sequencing of 16S rRNA gene

After MFCs were operated for 7 days post-inoculation plus 14 days of stability, anodic biofilm and supernatant DNA were sampled for genomic DNA extraction by using Powersoil DNA Isolation Kit (MO BIO Laboratories inc.), and DNA concentration was determined fluorometrically (Qubit® 3.0 dsDNA Broad Range Assay Kit, Life Technologies, Carlsbad, CA, USA).

All six resulting DNA samples were submitted to quantitative PCR of the 16S bacterial gene, using StepOne Real-Time PCR System (Applied Biosystems®) and primers P1 (5′ –CCCTACGGGAGGCAGCAG– 3′) and P2 (5′ –ATTACCGCGGCTGCTGG– 3′) (Muyzer et al., 1993).

The V4 region (length of ~373 bp) of bacterial 16S rRNA gene was amplified as described by and submitted to MiSeq sequencing. All sequence data were processed to remove adaptors using Scythe 0.991 and Cutadapt 1.7.1 (Martin, 2011), Sequence adjustment was performed by selecting sequences of >200 bp in length, with an average quality >20, based on Phred quality and how duplicate readings were removed using the Prinseq program (Schmieder et al., 2012). The QIIME version 1.9.1 software package was used to filter readings and determine Operating Taxonomic Units (OTUs) (Caporaso et al., 2011; Cole et al., 2014; Schmieder et al., 2012), using the Usearch algorithm to group OTU readings with 97% cutoff and to assign taxonomy using the Ribosomal Database Design (RDPII). Bacterial sequences were denatured and suspicious chimeras were removed using OTU tube function within QIIME. A representative sequence of each OTU was aligned for taxonomic identification using the SILVA database.

2.5. Determination of 16S rRNA gene copy number

To estimate the copy number of 16S rRNA gene present in eDNAs (environmental DNA) of samples, we used *Pseudomonas putida* 16S ribosomal gene as a marker. For this, we amplified *P. putida* KT2440 16S gene 1517 base pairs (bp) sequence using the oligonucleotides F27 (5'-AGAGTTTGA TCMTGGCTCAG-3′) and R1492 (5'-AGAGTTTGATCMTGGCTCAG-3′). Amplifications were performed at the following cycle steps: 95 °C – 1:00′, 50 °C – 30″ and 72 °C– 1:30′ in 35 cycles using GoTaq® DNA Polymerase (Promega). Amplicons were checked in agarose gel and posteriorly submitted to purification. The purified amplicons were cloned in pGEM-T Easy plasmid (Promega) (3015 bp) according to the manufacturer instructions and the final construct was subsequently used as DNA template for a quantitative PCR standard curve design. Reactions were performed using SsoFast™ EvaGreen® Supermix (Biorad) according to manufacturer instructions with 0.3 nM of primers P1 (5′ –CCCTACGGGAGGCAGCAG– 3′) and P2 (5′ –ATTACCGCGGCTGCTGG– 3′) (Muyzer et al., 1993). Determination of copy number was based on the product of the quantity of DNA (related to standard curve cycle threshold) and the Avogadro's number (6.022×10^{23}) divided by the product of the size of plasmid construct (bp) and the mean of molecular mass of 1 bp in double-strand DNA, equivalent to 660 Da, as performed by (de Azevedo et al., 2008). The results were expressed in copy number per gram of sample.

3. Results and discussion

3.1. Electricity generation and electrochemical activity of MFCs

Through simple voltage tracking, iron and sulfate supplementation kept power output profiles stable in the long-term operation of MFC (Fig. 1a). In the beginning, all MFCs showed similar cell voltage output (0.40 V), but the voltage of the MFC_A (MFC operating with the addition of acetate) dropped after the first few feeding cycles until 0.25 V. MFC_Fe (MFC running with addition of Fe_2O_3) and MFC_S (MFC working with addition of sulfate) presented stable cell voltage values. The average cell voltage during stable operation of MFC_S is slightly higher than MFC_Fe and MFC_A, respectively, 0.43 V and 0.39 V, and 0.35 V and are comparable with other works

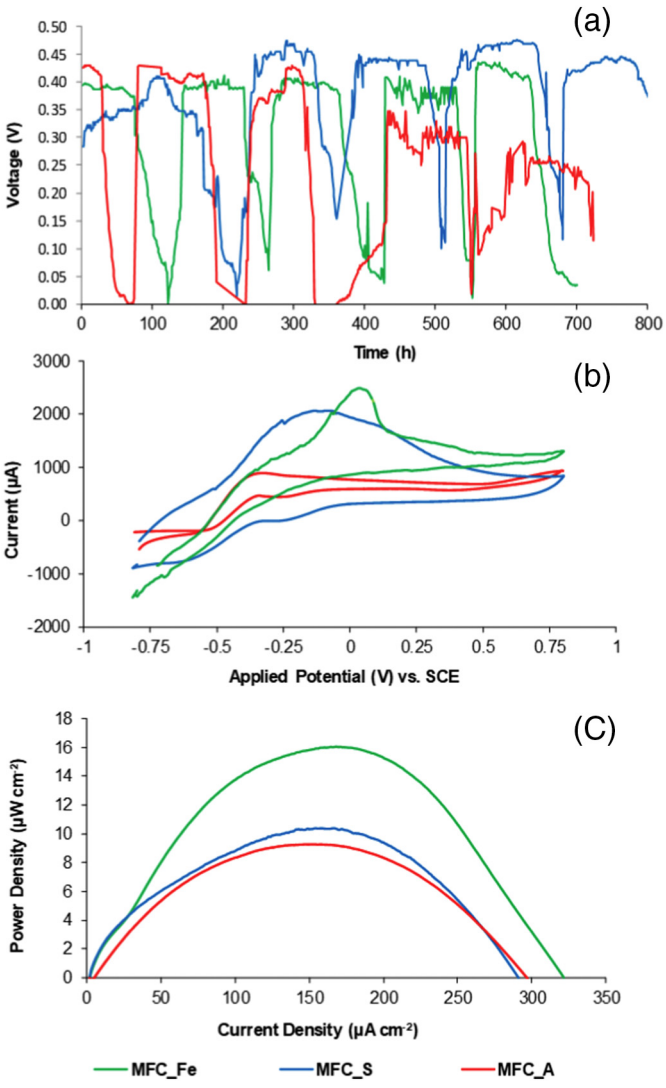

Fig. 1. (a) Cell voltage at 1000Ω during MFC operation fed with different culture media; (b) Cyclic voltammetric curves of the bioanodes operated at MFC on the 15th day fed with different inoculum. MFC_A with acetate alone; MFC_Fe with acetate and Fe_2O_3; and MFC_S with acetate and sulfate; (c) polarization curves for MFCs, correlating power densities with current intensity on the 15th day. MFC_A fed with acetate alone; MFC_Fe with acetate and Fe_2O_3; and MFC_S with acetate and sulfate.

(Kumar et al., 2017a; Lee et al., 2014b; Liu et al., 2017; Liu et al., 2018; Miran et al., 2017).

In comparison with the present state of the art, studies evaluating MFC scaling are increasing, and electrochemical constraints such as cathode activity, conductivity, and membrane performance are being strongly addressed, allowing remarkable performance. Despite their large volumes, pilot scale reactors can now achieve voltages between 0.3 V and 0.5 V (Hiegemann et al., 2019; Rossi et al., 2019). All in all, the voltages and currents here obtained were in accordance with the literature, not particularly impressive, as the average is around 0.45 V, although some studies reach 0.7 V, averages haven't surpassed these values in over a decade. However, the enquiring part was the metabolic network generating this electricity, which is discussed in the next sections.

The CV of the bioanodes (Fig. 1b) both show electroactivity of biofilms and reveals differences between the MFC treatments. All bioanodes presented an oxidation peak (MFC_A (−0.38 V vs. SCE), MFC_Fe (−0.038 V vs SCE) and MFC_S (− 0.10 V vs SCE).

The bioaonde in MFC_Fe presented a second peak, while the abiotic CV did not generate any peak, possibly because of Fe_2O_3 insolubility (Fig. S1). This anodic peak observed around 0.1 V vs SCE may be attributed to Fe^{2+} oxidation (McCafferty, 2010). The behavior of MFC_Fe is similar with other MFCs enriched with metals (Abbas et al., 2018; Alshahrani et al., 2019). The absence of the reduction peak of Fe^{3+} to Fe^{2+} in the reverse sweep suggests that the reduction occurs at more negative potentials.

The CV profile of MFC_S matches that seen in other sulfate-reducing communities fed with the same medium in literature, and reinforces that although the taxonomic composition differs, the functional groups may well be analogous (Kumar et al., 2017a). It also exhibits a possible reduction peak, indicative of a reversible reaction, whereby the sulfur might be cycled as a shuttle. This CV shows high capacitance and may be well related to the presence of a huge complex of interrelated hemes in sulfate reducers, connecting periplasmic redox proteins and acting as a capacitor for electron storage (Barton and Fauque, 2009; Heidelberg et al., 2004).

The bioelectrode in MFC_Fe also presented a second anodic peak (II) that might be related to iron species, while the abiotic CV did not generate any peak, possibly because of Fe_2O_3 insolubility (Fig. S1).

Polarization curves for all MFC investigated are shown in Fig. 1c, introduction of iron double the power density values compared to MFC_A.

The MFCs constructed for this study possessed a very low area to volume ratio (8 cm^2/200 cm^3). While most of the biofilm cells are associated to electricity generation, the suspended or planktonic cells are able to run more independent metabolisms and acting as primary step for degradation of complex pollutants. For example, in the MFC_Fe, the planktonic cells could access insoluble Fe_2O_3 to complete steps of iron cycling otherwise made difficult for the biofilm alone because of the frequent alternation of solid and soluble forms. However, the effects were very similar to those observed by Sangcharoen et al. (2015) (Sangcharoen et al., 2015), with a similar goal. The smallness of power outputs compared to polarization curve predictions (Fig. 1c) may be related to the large volume, which can promote more energetic balance between oxidizing and reducing nutrient cycling groups.

3.2. Microbial profiling of MFCs samples

In order to compare the microbial community of biofilms from MFCs with different compositions of ions, we use NGS targeting V4 hypervariable regions within microbial 16S rRNA genes. Approximately 1.7 million sequences corresponding to 4.94 Gbp of data from nine samples were generated. The average number of read-counts per sample was 34.621, ranging from 33.708 to 34.739. Thus, the data counts were normalized to 33.708 reads. After trimming, the final number of operational taxonomic units (OTU) consisted of 2032, 1750 e 2108 OTUs for MFC_A, MFC_F and MFC_S, respectively. Rarefaction curves based on the number of OTUs observed were comparably close to asymptotic for all samples, indicating that the analysis obtained enough readings to be representative of the sample's actual biodiversity (Fig. S2).

Analysis of samples from the MFCs biofilms showed a higher Shannon index a function correlated to species richness and diversity for MFC_S sample as compared to samples belonging to MFC_A and MFC_Fe (Kruskal-Wallis test, p-value $< .05$), the latter being the less diverse (Fig. 2a). Similar results were observed when the Simpson index was calculated, which serves as a species evenness indicator whose values are inversely related to biodiversity (Fig. 2b).

In all MFCs samples, Firmicutes and Proteobacteria accounted for >85% of phylum diversity, (49.7 ± 5.87% Firmicutes and 35 ± 4.47% Proteobacteria), being 96% of these Firmicutes of the Clostridia class (Fig. S3). MFC_Fe showed an increase in Betaproteobacteria over Firmicutes, while MFC_A had the lowest ratio. Proteobacteria and Firmicutes are well-known fermenters and syntrophic bacterial partners usually behaving as Anode Respiring Bacteria (ARB) and fermenter, respectively (Freguia et al., 2010; Kiely et al., 2011). Bacteroidetes (6.4 ± 0.56%) has been associated with biofilm anodes, but with low fractions of total Bacteria which is in accordance with this study (Torres et al., 2007; Xing et al., 2008). Euryachaeota and Tenericutes constituted < 1%. Synergistetes was present only in MFC_S (0.7%).

Furthermore, 16S rRNA gene copy abundance analysis revealed a much higher bacterial population on the MFC_A biofilm, which might be related to the lower observed voltages because biofilm thickness can impair electron diffusion through the EPS to the electrode by increasing resistance (Fig. 3) (Lee et al., 2014b). MFC_Fe showed a slightly larger number of copies in the supernatant, followed by MFC_S (although Tukey HSD test achieved Q statistic and p-value of 3.8963 and 0.1362516, respectively) which could be associated to a larger involvement of planktonic cells in energy generation, for example by adhesion of cells to the insoluble iron oxide to reduce it, or shuttle-producers in MFC_S, and also greater homoacetogenic activity, which is dominated by planktonic cells (Fig. 3).

Given that this is one of the first bioanode communities derived from the marine sediment of a Southern Hemisphere region, it is clear that the overall composition differs greatly from any previously described in literature, both by the lack of the ubiquitous model ARB and by the large number of Not Assigned OTUs (MFC_A 5.8%; MFC_Fe 3.9%; MFC_S 13%), indicating a large potential of novel biodiversity to be explored from the inoculum (Ruiz et al., 2014). Most other studies report a core microbiome starred by *Geobacter, Shewanella, Arcobacter,* or *Desulfuromonas*, even in the presence of sulfur or iron (Call et al., 2009)–(Parameswaran et al., 2009a), while this study located none of these traditional groups above the 0.1% threshold besides *Desulfuromonas*, and rather has found a larger importance of *Desulfomicrobium* and other groups not traditionally affiliated with microbial fuel cell bioanodes (Fig. 2c). Previous works reported in the literature have shown that novel biofilms were replaced by *Geobacter* dominance after longer periods of time (Lovley, 1993; Lovley and Phillips, 1988). However, biofilms studied in this work presented absolutely no Geobacteraceae above the threshold of detection, making the chances of such dominance replacement very unlikely.

The unusual characteristics of this biofilm are consistent with findings from the previous study conducted on the same inoculum with different 16S amplicon study methodology and operating conditions (Dos Passos et al., 2019), reinforcing the contrast starkness relative to other literature. Although the different treatments in this study did seem to produce communities slightly different between themselves, the ten most prevalent groups remained the same in all three MFCs (together representing on average 78% of the biofilm composition (Fig. 2c and Table S1), with minute deviations between absolute abundances.

Core microbiome analysis showed that 17 genera were shared in the three samples at the minimum detection threshold of 0.001% (Fig. 4a, b, and c). Accordingly, the core microbiome characteristic of this Southern Hemisphere sediment was formed by *Clostridium, Desulfomicrobium, Advenella, Tindallia, Parabacteroides, Sedimentibacter, Desulfuromonas, Pseudomonas, Eubacterium, Tissierella, Trichococcus, Azospira, Thauera, Erysipelothrix, Alkaliphilus, Delftia,* and *Azoarcus* at the detection threshold of 0.001% (Fig. 4a-c).

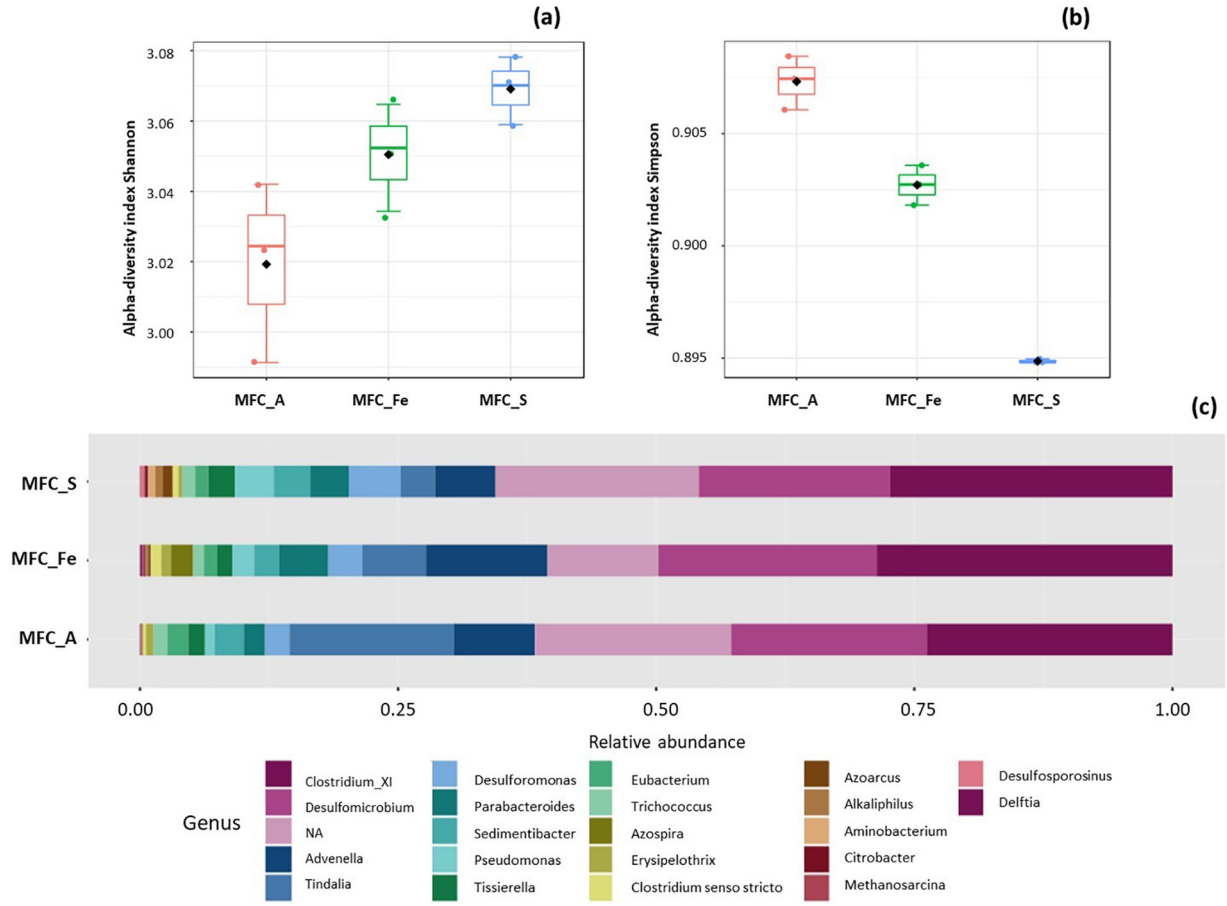

Fig. 2. a) Alpha diversity at OTU level at Acetate (red, $n = 16$), Iron (green, n = 16) and Sulfate (blue, n = 16) calculated using Simpson and Shannon indexes (Kruskal-Wallis test, p-value $< .05$). b) Relative abundance of each taxon in bioanodes from MFC_A, MFC_Fe, and MFC_S at genera level.

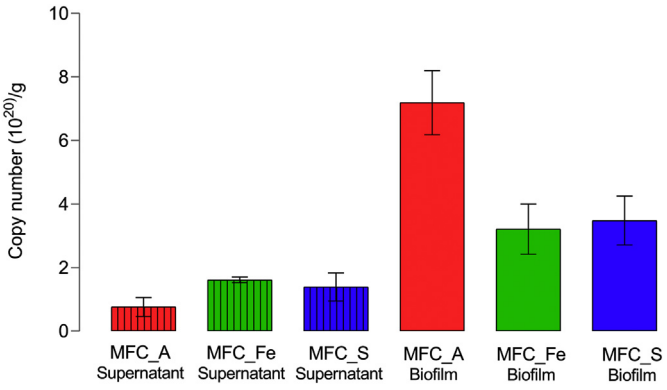

Fig. 3. 16S rRNA gene copy abundance in each of the MFC biofilms and supernatant.

Considering this scenario although the power-generating behavior was different, especially between MFC_A and the other two conditions, the microbial communities composing the biofilms were very similar, meaning that the electrochemical differences are probably due to: i) the small but significant shifts in community composition, or ii) metabolic shifts that allow the same microorganisms to perform differential functions affecting power generation given environmental changes. These may include, but are not limited to, enrichment of bacteria with alternative metabolic pathways capable of dissimilatory metal-reducing, polyvalent ion intake, denitrifying sulfide removal, insertion of competitive ions into the electron transport cycle, coupling to nitrate respiration, for example, through sulfate cycling or Feammox metabolisms, which will be further discussed. Although MFC_Fe and MFC_S both generated similar power, they were not the most similar microbiologically (Fig. 5 and S4).

This is consistent with the fact that the medium compositions for MFC_Fe and MFC_A were more similar than MFC_S, because of adaptations that would make sulfate ions more accessible (Postgate, 1979), and reinforces that the differences between biofilms were most probably caused by the media.

3.3. Ecologic networks of microbial communities in MFCs

Many studies investigating community structure in MFCs find a general organization composed by the three-way syntrophy (Parameswaran et al., 2009a): fermenters, hydrogen scavengers, and ARB, which are typically composed, respectively, by *Clostridia* or *Eubacterium*; hydrogenotrophic methanogenic archaea, homoacetogens, or hydrogen consuming ARB; and the other ARB already cited (Ruiz et al., 2014). Thus, this model has served as a template for the drafting of the microbial community structure observed from this inoculum, where the fermentation niche mainly composed by Stickland Fermenters (*Tindallia, Parabacteroides, Sedimentibacter*) and *Desulfomicrobium*, the Hydrogen Scavenging niche composed by Homoacetogens (*Clostridia* and *Eubacterium),* and the ARB niche being filled by *Pseudomonas, Desulfuromonas, Tissierella* (Fig. 4, and Table S1).

Many groups are capable of Stickland fermentation *(Clostridium XI, Tindallia, Sedimentibacter, and Parabacteroides*) (Table S1), by converting amino acids to acetate and ammonium (Buchanan et al., 1975; Pikuta,

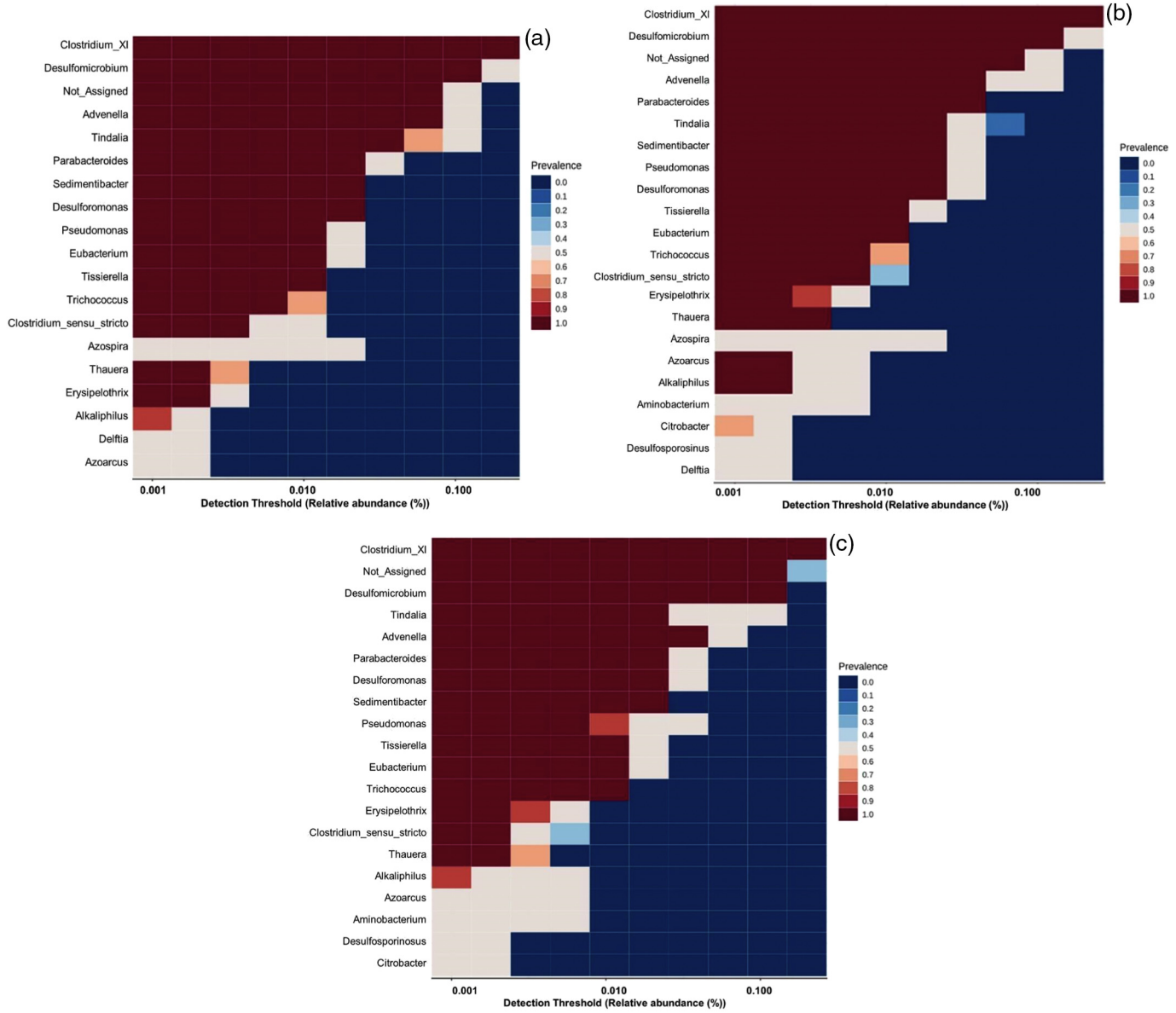

Fig. 4. Core microbiome analysis based on relative abundance and sample prevalence of bacterial genera in (a) MFC_A and MFC_Fe (b) MFC_A and MFC_S (c) MFC_S and MFC_Fe.

2015). This pathway was probably executed jointly with homoacetogenesis in some cases (Faust and Raes, 2012). Dominance of these groups may be related to the large amount of inoculating material, which suffered great selective pressures during start-up, generating a large amount of dead cells and thus favoring groups related to cell decomposition such as Stickland fermenters. It would also explain the increase in reactor pH, from 6.5 to about 8.5 every week. However, alkaline pH constitutes a challenging environment for dissimilatory metal-reducing bacteria as it is difficult to maintain a proton-motive force across the cell membrane when the external pH exceeds that of the cytoplasm, which may favor fermentative metabolism over respiration because they don't depend on proton-motive-force (Fuller et al., 2015; Miller et al., 2010). This may also be related to a large amount of acetate regeneration, considering that the alkaline environment favors reductive bioreactions (totaling at least 61.8%).

Desulfomicrobium, on the other hand, probably converted intermediate alcohols to acetate coupled with exoelectrogenesis. The dominance of *Desulfomicrobium* is particularly impressive, considering that this genus is incapable of growing using acetate or other organic acids, being rather associated with its formation (Genthner et al., 2015; Thevenieau et al., 2007).

Tindallia is capable of Stickland fermentation, along with acetate consumption, thiosulfate reduction, homoacetogenesis, and/or Fe (III) reduction (evidence of the genus' metabolic versatility) (Pikuta, 2015). However, its scarcity in MFC literature and its metabolic versatility make it hard to be categorized into a single functional group. The ability to reduce iron, along with its phylogenetic relation to known exoelectrogen *Alkaliphilus* (Flayac et al., 2018), suggests that this *Tindallia* may also be exoelectrogenic.

The structure and behavior of fermenters in this biofilm were very distinct than others found in similar studies, mainly because other fermenters reported in literature typically ferment sugars into acids, whereas this community represents a marine ecosystem (adapted to decomposition where sugars are not readily available).

Approximately 30% of the community is capable of performing homoacetogenesis (*Clostridia* and *Eubacteria*), indicates the significant formation of CO_2 and H_2 around the biofilm. Although GC analysis only detected H_2 in MFC_Fe (data not shown), it is known that anode-produced H_2 is consumed locally before becoming gas, either oxidized to reduce iron or forming methane (also detected) (Table 1). Homoacetogenic

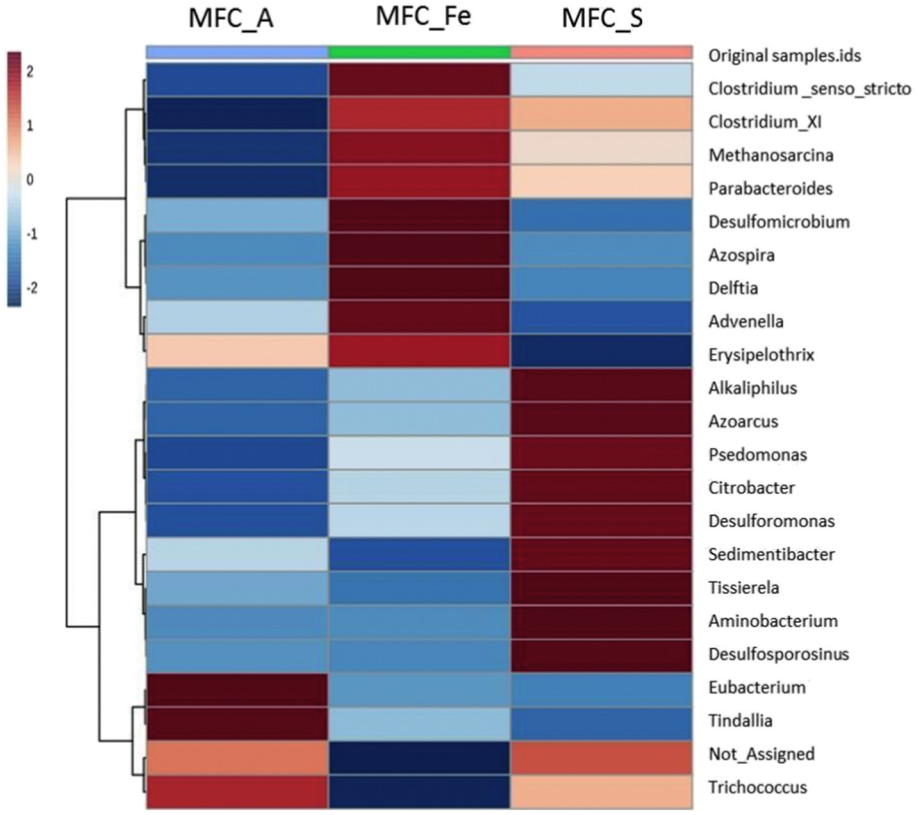

Fig. 5. Clustering analysis of the MFC_A, MFC_Fe, and MFC_S. (a) Heatmap, and hierarchical clustering of the main genera associated with MFC_A, MFC_Fe, and MFC_S samples. The heatmap shows the relative abundance of top 22 bacterial genera (rows) in each sample (columns). Hierarchical clustering is based on the Ward Clustering algorithm and Euclidean Distance measure to generate the hierarchical tree. The color bar indicates the range of the relative abundance.

hydrogen-scavenging is capable of recovering much more oxidation energy than alternative pathways, and, by participating as a key cofactor in electron-transportases and hydrogenases, iron supplementation has been suggested to stimulate this behavior (Parameswaran et al., 2009b; Zhang et al., 2019). Some groups such as *Acidithiobacillus ferrooxidans* can also oxidize hydrogen for ferric iron reduction, and although this group was not detected, hydrogen presence might serve as a substrate for ferric reduction by bacteria in MFC_Fe.

A few known methanogens were detected (*Methanosarcina)*, although methane was below the detection limit. *Methanosarcina* have been shown to be capable of extracting electrons both from conductive surfaces (ie. the anode) and through interspecies electron transfer with electrogens, acting as an electron pirate within MFCs (Yee et al., 2019). The low abundance may be explained by the exposure of anodes to air when the new substrate was added, causing inhibition to anaerobic methanogens, limiting its proliferation and methane accumulation, as described by (Ruiz et al., 2014).

Among the acetate consumers, *Tissierella* and *Pseudomonas* produce electron shuttles such as riboflavin and pyocyanin, respectively, thus participating in electricity generation. *Desulfuromonas* are acetate-consuming exoelectrogens by direct contact, found extensively in MFCs. *Advenella* is a sulfate oxidizing group (or, in sulfate-free cells, probably anode oxidizing).

Tindallia and *Advenella* both represent groups never before associated with MFCs or exoelectrogenesis, but rather with soda ponds and sulfate cycling. In addition, they do not even seem to grow at pH below 7.5. The

Table 1
Chemical characterization and consumption of compounds during a cycle of MFCs operation.

MFC	MN	Ammonium (mg/L)	Nitrite (mg/L)	Nitrate (mg/L)	Sulfate (mg/L)	Acetate (mg/L)
	Initial	471.4 ± 0.002	17.2 ± 0.001	< DL	2.0 ± 0.001	1183 ± 0.005
	Final	349.7 ± 0.001	14.8 ± 0.002	< DL	< DL	482.0 ± 0.002
MFC_A	Consumption (mg/L)	121.7	2.4	< DL	2.0	700.9
	Consumption (%)	25.8	13.9	–	100.0	59.3
	Initial	388.1 ± 0.002	20.1 ± 0.0015	< DL	2.8 ± 0.0005	1185.9 ± 0.003
	Final	132.1 ± 0.003	17.1 ± 0.003	85.9	1.9 ± 0.003	922.0 ± 0.001
MFC_Fe	Consumption (mg/L)	255.9	2.9	−85.9	0.9	263.9
	Consumption (%)	66.0	14.7	–	32.4	22.3
	Initial	339.3 ± 0.008	>LD	< DL	600.8 ± 0.002	1202.9 ± 0.001
	Final	327.4 ± 0.002	20.1 ± 0.001	< DL	555.5 ± 0.001	80.8 ± 0.0025
MFC_S	Consumption (mg/L)	11.9	−20.1	< DL	45.2	1122.2
	Consumption (%)	3.5	–	–	7.5	93.38

< DL indicates below detection limit.

dominance of *Advenella* is indirect evidence of sulfate reoxidation in MFC_S and nitrate to nitrite conversion in MFC_Fe, using it as a final acceptor (Ghosh and Dam, 2009). Similarly, other microorganisms which belong to the same order and with homologous sulfate oxidation pathway (ie. *Thiobacillus)* are also able to oxidize Fe^{2+}, explaining their role in MFC_Fe (Fukushima et al., 2015), especially considering the already mentioned difficulty of dissimilatory metal-reduction in alkaline conditions, which would favor a alkaliphile such as *Advenella* for this function. The generalized dominance of sulfate-cycling groups most probably replaced sulfate with the anode as electron-sink in MFC_A and MFC_Fe (Table S1).

It is also relevant to note that although nitrate and sulfate can both act as an exogenous electron sink similarly competing with the anode (by acting as final electron acceptor to sulfate-reducers and Feammox/nitrifiers, they did not seem to outcompete the anode when formed in MFC_Fe, or when added to MFC_S, since as they still showed greater power outputs than MFC_A (which lacked sulfate and nitrate).

Determinations of the different iron forms (Table S2) show that, as expected, only a small amount of the iron was solubilized (6.6%), but of this portion, 91% was in the form Fe^{2+}. In the observed pH and voltages, Fe^{3+} form is disadvantaged, and Fe^{2+}, when reoxidized, mostly returns to Fe_2O_3, which hinders its role as a mediator due to insolubilization and lower accessibility after reoxidation. Reoxidation of the solubilized iron occurs very easily, especially considering that iron-oxidizing bacteria are able to oxidize it at a 50×10^3 times faster rate than the chemical reaction (Singh et al., 2018), including bacteria seen in the MFCs of this study such as *Pseudomonas* (Liu et al., 2013). In any case, all iron redox reactions have reduction or oxidation potentials within the capabilities of MFCs (Encyclopedia of Inorganic Chemistry, 2006).

The total nitrogen consumption indicates the importance of nitrogen cycling and the differences among the bioanodic metabolisms. MFC_A nitrogen consumption is similar to literature reports, between 15 and 20%, while MFC_S seemed to have ammonia consumption inhibited, and MFC_Fe presented a threefold increase compared to the literature average (Hiegemann et al., 2019) (Table 1).

MFC_Fe stood out for its low acetate consumption, but also with its large nitrate production (Table 1). Nitrate concentrations correspond precisely to ammonium consumption. It is possible, therefore, that a significant part of the energy produced by MFC_Fe that is not explained by the electrons from acetate oxidation is related to the energy obtained from nitrite to nitrate oxidation, coupled with Fe (III) reduction, deemed Feammox (Ruiz-Urigüen et al., 2018b).

The decrease in the electroactive acetogen and incomplete-oxidizing sulfate-reducer *Desulfomicrobium* in the presence of sulfate was unexpected, while general ARB such as *Desulfuromonas, Pseudomonas,* and *Tissierella* increased (Fig. 2c and Table S1). Thus, electricity generation in MFC_S was much more dependent on acetate consumption (Table 1), while in other reactors it was dominated by *Desulfomicrobium*. Simultaneously, MFC_S showed a decrease in most fermenters and homoacetogens.

The sulfur oxidizers were *Advenella*, which obtained the lowest abundances in MFC_S (5.6% compared to 7.6% in MFC_A and maximum 11.3% in MFC_Fe) (Fig. 5 and Table S1). *Tindallia* also drastically diminished in MFC_S and both are alkaliphiles, so it is possible that the pH conditions made sulfur precipitation unfavorable. As a matter of fact, Zheng and colleagues (Zheng et al., 2014) have already shown that biofilms at a pH of 8.5 remove less than half of the sulfate amount when compared to lower pHs. Another possible explanation for the low sulfate removal in this system is that a portion of sulfide was reoxidized to sulfate, not sulfur, as already described in other works (Cai and Zheng, 2013; Habermann and Pommer, 1991; Sangcharoen et al., 2015). Although sulfur oxidizers *Advenella* decreased in abundance, other organisms may have filled this role; for instance, *Pseudomonas* has also been shown to include sulfur-oxidizing bacteria and showed an increase in MFC_S (Sun et al., 2009). If so, the in-situ generated sulfide acts as an electron donor during its oxidation to sulfate, closing the sulfur cycle and potentially acting as an inorganic electron shuttle. On one hand, this means that sulfate was not efficiently removed as a pollutant from this synthetic wastewater in MFC_S, but on the other, it shows that its cycling can still raise electricity production by facilitating electron transfer (Alexandrino et al., 2014a) also describes a syntrophic partnership between *Clostridia* and SRB, but which may have been thrown off-balance in MFC_S.

4. Conclusions

This study has produced and analyzed a bioanode grown from Southern Hemisphere marine sediment and, in it, observed a completely novel type of community structure, missing in traditional exoelectrogens organisms, such as *Geobacter*, while being also rich in unusual species. The nutritional monitoring observed here suggests activation of different metabolic pathways within the same community, without greatly altering biodiversity or core community composition, which allowed the MFCs to have distinct electrochemical behaviors.

Data Availability

The nucleotide sequences obtained in the present study have been deposited in the GenBank database under the accession number PRJNA591302.

Funding

This work was supported by the São Paulo State Foundation for Research Aid (FAPESP, grant numbers 2018/15528–4, 2018/12471, and 2018/00789–7) and by the Young Research Award by the Sao Paulo State Foundation (FAPESP, award number 2015/04309–1). LBKM, LM, and GMVS are beneficiaries of FAPESP fellowships (award numbers 2018/15528–4, 2016/18827–7 and 2018/072618 respectively).

Author Contributions

Lucca Bonjy Kikuti Mancilio, Valeria Reginatto, and María-Eugenia Guazzaroni conceived of the project and wrote the final manuscript. Guilherme Augusto Ribeiro and Adalgisa Rodrigues Andrade helped by electrochemical analysis and discussion.

Lucca Bonjy Kikuti Mancilio, Leonardo Martins-Santana, and Guilherme Marcelino Viana de Siqueira conducted the nucleic acid extractions and contributed to the data analysis. Erica Mendes Lopes and Luciano Takeshi Kishi conducted the MiSeq library preparations and provided bioinformatics support. All authors have read and approved the manuscript.

Declaration of competing interest

The authors declared that they had no conflicts of interest with respect to their authorship or the publication of this article.

Appendix A. Supplementary data

Supplementary data to this article can be found online at https://doi.org/10.1016/j.crbiot.2020.04.001.

References

Abbas, S.Z., Rafatullah, M., Ismail, N., Shakoori, F.R., 2018. Electrochemistry and microbiology of microbial fuel cells treating marine sediments polluted with heavy metals. RSC Advances 8 (34), 18800–18813. https://doi.org/10.1039/c8ra01711e.

Alexandrino, M., Costa, R., Canário, A.V.M., Costa, M.C., 2014a. Clostridia Initiate Heavy Metal Bioremoval in Mixed Sulfidogenic Cultures. Environ. Sci. Technol. 48 (6), 3378–3385. https://doi.org/10.1021/es4052044.

Alshahrani, A., Fitch, A., Al-Bazi, J., 2019. Metal Ions Impact on *Shewanella Oneidensis* MR-1 Adhesion to ITO Electrode and the Enhancement of Current Output. American Journal of Analytical Chemistry 10 (09), 428–443. https://doi.org/10.4236/ajac.2019.109031.

Barton, L.L., Fauque, G.D., 2009. Chapter 2 Biochemistry, Physiology and Biotechnology of Sulfate-Reducing Bacteria. Advances in Applied Microbiology., 41–98 https://doi.org/10.1016/s0065-2164(09)01202-7.

Buchanan, F.A.S., Gibbons, R.T.E., Bergey, N.E., 1975. Bergey's Manual of Determinative Bacteriology. Taxon 24 (2/3), 377. https://doi.org/10.2307/1218353.

Cai, J., Zheng, P., 2013. Simultaneous anaerobic sulfide and nitrate removal in microbial fuel cell. Bioresour. Technol. 128, 760–764 Jan.
Call, D.F., Wagner, R.C., Logan, B.E., 2009. Hydrogen Production by Geobacter Species and a Mixed Consortium in a Microbial Electrolysis Cell. Applied and Environmental Microbiology 75 (24), 7579–7587. https://doi.org/10.1128/aem.01760-09.
Caporaso, J.G., Lauber, C.C., Walters, W.A., Berg-Lyons, D., Lozupone, C.A., Turnbaugh, P.J, et al., 2011. Global patterns of 16S rRNA diversity at a depth of millions of sequences per sample. Proc. Natl. Acad. Sci. U. S. A. 108 (Suppl 1), 4516–4522 Mar.
Clesceri, L.S., American Public Health Association, 2005. Standard Methods for the Examination of Water & Wastewater. Ignatius Press.
Cole, J.R., Fish, J.A., Chai, B., McGarrel, D.M., Sun, Y., Wang, Q., et al., 2014. Ribosomal Database Project: data and tools for high throughput rRNA analysis. Nucleic Acids Res. 42 (Database issue), D633–42 Jan.
Cvetkovic, A., Menon, A.L., Thorgersen, M.P., Scott, J.W., Poole 2nd, F.L, Jenney Jr., F.E., et al., 2010. Microbial metalloproteomes are largely uncharacterized. Nature 466 (7307), 779–782 Aug.
Daghio, M., Vaiopoulou, E., Aulenta, F., Sherry, A., Head, I., Franzetti, A., et al., 2018. Anode potential selection for sulfide removal in contaminated marine sediments. J. Hazard. Mater. 360, 498–503. https://doi.org/10.1016/j.jhazmat.2018.08.016.
de Azevedo, J.S.N., Silva-Rocha, R., Silva, A., Carepo, M.S.P., Schneider, M.P.C., 2008. Gene expression of the arsenic resistance operon in Chromobacterium violaceum ATCC 12472. Canadian Journal of Microbiology 54 (2), 137–142. https://doi.org/10.1139/w07-123.
Dos Passos, V.F., Marcilio, R., Aquino-Neto, S., Santana, F.B., Dias, A.C.F., Andreote, F.D., et al., 2019. Hydrogen and electrical energy co-generation by a cooperative fermentation system comprising Clostridium and microbial fuel cell inoculated with port drainage sediment. Bioresour. Technol. 277, 94–103 Apr.
dos Reis, D.C.O., 2016. Caracterização dos íons majoritários do material particulado da atmosfera de Ribeirão Preto, uma cidade canavieira do estado de São Paulo. https://doi.org/10.11606/d.59.2016.tde-21102016-1020251.
Pourbaix Diagram. Encyclopedia of Inorganic Chemistry https://doi.org/10.1002/0470862106.id659.
Faust, K., Raes, J., 2012. Microbial interactions: from networks to models. Nature Reviews Microbiology 10 (8), 538–550. https://doi.org/10.1038/nrmicro2832.
Flayac, J.-C., Trably, E., Bernet, N., 2018. Microbial Ecology of Anodic Biofilms: From Species Selection to Microbial Interactions. Microbial Fuel Cell., 63–85 https://doi.org/10.1007/978-3-319-66793-5_4.
Freguia, S., Teh, E.H., Boon, N., Leung, K.M., Keller, J., Rabaey, K., 2010. Microbial fuel cells operating on mixed fatty acids. Bioresource Technology 101 (4), 1233–1238. https://doi.org/10.1016/j.biortech.2009.09.054.
Fukushima, J., Tojo, F., Asano, R., Kobayashi, Y., Shimura, Y., Okano, K., et al., 2015. Complete Genome Sequence of the Unclassified Iron-Oxidizing, Chemolithoautotrophic Burkholderiales Bacterium GJ-E10, Isolated from an Acidic River. Genome Announc. 3 (1). https://doi.org/10.1128/genomeA.01455-14 Feb.
Fuller, S.J., Burke, I.T., McMillan, D.G.G., Ding, W., Stewart, D.I., 2015. Population Changes in a Community of Alkaliphilic Iron-Reducing Bacteria Due to Changes in the Electron Acceptor: Implications for Bioremediation at Alkaline Cr(VI)-Contaminated Sites. Water Air Soil Pollut. 226 (6). https://doi.org/10.1007/s11270-015-2437-z.
Gajda, I., Greenman, J., Ieropoulos, I.A., 2018. Recent advancements in real-world microbial fuel cell applications. Curr Opin Electrochem 11, 78–83 Oct.
Genthner, B.R.S., Sharak Genthner, B.R., Devereux, R., 2015. Desulfomicrobium. Bergey's Manual of Systematics of Archaea and Bacteria., 1–9 https://doi.org/10.1002/9781118960608.gbm01032.
Ghosh, W., Dam, B., 2009. Biochemistry and molecular biology of lithotrophic sulfur oxidation by taxonomically and ecologically diverse bacteria and archaea. FEMS Microbiology Reviews 33 (6), 999–1043. https://doi.org/10.1111/j.1574-6976.2009.00187.x.
Habermann, W., Pommer, E.H., 1991. Biological fuel cells with sulphide storage capacity. Appl. Microbiol. Biotechnol. 35 (1). https://doi.org/10.1007/bf00180650.
Heidelberg, J.F., et al., 2004. The genome sequence of the anaerobic, sulfate-reducing bacterium Desulfovibrio vulgaris Hildenborough. Nat. Biotechnol. 22 (5), 554–559 May.
Hiegemann, H., et al., 2019. Performance and inorganic fouling of a submergible 255 L prototype microbial fuel cell module during continuous long-term operation with real municipal wastewater under practical conditions. Bioresour. Technol. 294, 122227. https://doi.org/10.1016/j.biortech.2019.122227.
Janicek, A., Fan, Y., Liu, H., 2014. Design of microbial fuel cells for practical application: a review and analysis of scale-up studies. Biofuels 5 (1), 79–92. https://doi.org/10.4155/bfs.13.69.
Kiely, P.D., Rader, G., Regan, J.M., Logan, B.E., 2011. Long-term cathode performance and the microbial communities that develop in microbial fuel cells fed different fermentation endproducts. Bioresource Technology 102 (1), 361–366. https://doi.org/10.1016/j.biortech.2010.05.017.
Kisch, J.M., Utpatel, C., Hilterhaus, L., Streit, W.R., Liese, A., 2014. *Pseudomonas aeruginosa* Biofilm Growth Inhibition on Medical Plastic Materials by Immobilized Esterases and Acylase. Chem. Bio. Chem. 15 (13), 1911–1919. https://doi.org/10.1002/cbic.201400023.
Kumar, S.S., Malyan, S.K., Basu, S., Bishnoi, N.R., 2017a. Syntrophic association and performance of Clostridium, Desulfovibrio, Aeromonas and Tetrathiobacter as anodic biocatalysts for bioelectricity generation in dual chamber microbial fuel cell. Environ. Sci. Pollut. Res. Int. 24 (19), 16019–16030 Jul.
Lee, D.-J., Liu, X., Weng, H.-L., 2014b. Sulfate and organic carbon removal by microbial fuel cell with sulfate-reducing bacteria and sulfide-oxidising bacteria anodic biofilm. Bioresour. Technol. 156, 14–19 Mar.
Liu, Q., Guo, H., Li, Y., Xiang, H., 2013. Acclimation of arsenic-resistant Fe(II)-oxidizing bacteria in aqueous environment. Int. Biodeterior. Biodegrad. 76, 86–91. https://doi.org/10.1016/j.ibiod.2012.06.018.
Liu, Q., Liu, B., Li, W., Zhao, X., Zuo, W., Xing, D., 2017. Impact of Ferrous Iron on Microbial Community of the Biofilm in Microbial Fuel Cells. Front. Microbiol. 8, 920 Jun.
Liu, Q., Yang, Y., Mei, X., Liu, B., Chen, C., Xing, D., 2018. Response of the microbial community structure of biofilms to ferric iron in microbial fuel cells. Science of The Total Environment 631–632, 695–701. https://doi.org/10.1016/j.scitotenv.2018.03.008.
Logan, B.E., 2008. Microbial Fuel Cells. John Wiley & Sons.
Logan, B.E., Regan, J.M., 2006. Electricity-producing bacterial communities in microbial fuel cells. Trends Microbiol. 14 (12), 512–518 Dec.
Lovley, D.R., 1993. Anaerobes into heavy metal: Dissimilatory metal reduction in anoxic environments. Trends Ecol. Evol. 8 (6), 213–217 Jun.
Lovley, D.R., Phillips, E.J., 1988. Novel mode of microbial energy metabolism: organic carbon oxidation coupled to dissimilatory reduction of iron or manganese. Appl. Environ. Microbiol. 54 (6), 1472–1480 Jun.
Lu, Z., Chang, D., Ma, J., Huang, G., Cai, L., Zhang, L., 2015. Behavior of metal ions in bioelectrochemical systems: A review. J. Power Sources 275, 243–260. https://doi.org/10.1016/j.jpowsour.2014.10.168.
Martin, M., 2011. Cutadapt removes adapter sequences from high-throughput sequencing reads. EMBnet.journal 17 (1), 10. https://doi.org/10.14806/ej.17.1.200.
Matturro, B., Cruz Viggi, C., Aulenta, F., Rossetti, S., 2017. Cable Bacteria and the Bioelectrochemical Snorkel: The Natural and Engineered Facets Playing a Role in Hydrocarbons Degradation in Marine Sediments. Front. Microbiol. 8, 952 May.
McCafferty, E., 2010. Thermodynamics of Corrosion: Pourbaix Diagrams. Introduction to Corrosion Science., 95–117 https://doi.org/10.1007/978-1-4419-0455-3_6.
Mei, X., Guo, C., Liu, B., Tang, Y., Xing, D., 2015. Shaping of bacterial community structure in microbial fuel cells by different inocula. RSC Advances 5 (95), 78136–78141. https://doi.org/10.1039/c5ra16382j.
Miller, L.D., Mosher, J.J., Venkateswaran, A., Yang, Z.K., Palumbo, A.V., Phelps, T.J., et al., 2010. Establishment and metabolic analysis of a model microbial community for understanding trophic and electron accepting interactions of subsurface anaerobic environments. BMC Microbiol. 10 (1), 149. https://doi.org/10.1186/1471-2180-10-149.
Miran, W., Jang, J., Nawaz, M., Shahzad, A., Jeong, S.E., Jeon, C.O., et al., 2017. Mixed sulfate-reducing bacteria-enriched microbial fuel cells for the treatment of wastewater containing copper. Chemosphere 189, 134–142. https://doi.org/10.1016/j.chemosphere.2017.09.048.
Mohan, S.V., Venkata Mohan, S., Velvizhi, G., Annie Modestra, J., Srikanth, S., 2014. Microbial fuel cell: Critical factors regulating bio-catalyzed electrochemical process and recent advancements. Renew. Sust. Energ. Rev. vol. 40, 779–797. https://doi.org/10.1016/j.rser.2014.07.109.
Muyzer, G., de Waal, E.C., Uitterlinden, A.G., 1993. Profiling of complex microbial populations by denaturing gradient gel electrophoresis analysis of polymerase chain reaction-amplified genes coding for 16S rRNA. Appl. Environ. Microbiol. 59 (3), 695–700 Mar.
Parameswaran, P., Torres, C.I., Lee, H.-S., Krajmalnik-Brown, R., Rittmann, B.E., 2009a. Syntrophic interactions among anode respiring bacteria (ARB) and Non-ARB in a biofilm anode: electron balances. Biotechnology and Bioengineering 103 (3), 513–523. https://doi.org/10.1002/bit.22267.
Parameswaran, P., Torres, C.I., Lee, H.-S., Krajmalnik-Brown, R., Rittmann, B.E., 2009b. Syntrophic interactions among anode respiring bacteria (ARB) and Non-ARB in a biofilm anode: electron balances. Biotechnology and Bioengineering 103 (3), 513–523. https://doi.org/10.1002/bit.22267.
Perazzoli, S., Bastos, R.B., Santana, F.B., Soares, H.M., 2018. Biological fuel cells produce bioelectricity with in-situ brackish water purification. Water Sci. Technol. 78 (1–2), 301–309 Aug.
Pikuta, E.V., 2015. Tindallia. Bergey's Manual of Systematics of Archaea and Bacteria., 1–8 https://doi.org/10.1002/9781118960608.gbm00625.
Postgate, J.R., 1979. The Sulphate-Reducing Bacteria. CUP Archive. .
Rossi, R., et al., 2019. Evaluating a multi-panel air cathode through electrochemical and biotic tests. Water Res. 148, 51–59 Jan.
Ruiz, V., Ilhan, Z.E., Kang, D.-W., Krajmalnik-Brown, R., Buitrón, G., 2014. The source of inoculum plays a defining role in the development of MEC microbial consortia fed with acetic and propionic acid mixtures. J. Biotechnol. 182–183, 11–18. https://doi.org/10.1016/j.jbiotec.2014.04.016.
Ruiz-Urigüen, M., Shuai, W., Jaffé, P.R., 2018a. Electrode Colonization by the Feammox Bacterium Acidimicrobiaceae sp. Strain A6. Appl. Environ. Microbiol. 84 (24). https://doi.org/10.1128/aem.02029-18.
Ruiz-Urigüen, M., Shuai, W., Jaffé, P.R., 2018b. Feammox Acidimicrobiaceae bacterium A6, a lithoautotrophic electrode-colonizing bacterium. https://doi.org/10.1101/300731.
Sangcharoen, A., Niyom, W., Suwannasilp, B.B., 2015. A microbial fuel cell treating organic wastewater containing high sulfate under continuous operation: Performance and microbial community. Process Biochemistry 50 (10), 1648–1655. https://doi.org/10.1016/j.procbio.2015.06.013.
Schmieder, R., Lim, Y.W., Edwards, R., 2012. Identification and removal of ribosomal RNA sequences from metatranscriptomes. Bioinformatics 28 (3), 433–435 Feb.
Sharma, S.C.D., Feng, C., Li, J., Hu, A., Wang, H., Qin, D., et al., 2016. Electrochemical Characterization of a Novel Exoelectrogenic Bacterium Strain SCS5, Isolated from a Mediator-Less Microbial Fuel Cell and Phylogenetically Related to *Aeromonas jandaei*. Microbes Environ. 31 (3), 213–225 Sep.
Singh, V.K., Singh, A.L., Singh, R., Kumar, A., 2018. Iron oxidizing bacteria: insights on diversity, mechanism of iron oxidation and role in management of metal pollution. Environ. Sustain. 1 (3), 221–231. https://doi.org/10.1007/s42398-018-0024-0.
Sun, M., Mu, Z.X., Chen, Y.P., Sheng, J.P., Liu, X.W., Chen, Y.Z., et al., 2009. Microbe-assisted sulfide oxidation in the anode of a microbial fuel cell. Environ. Sci. Technol. 43 (9), 3372–3377 May.
Thevenieau, F., Fardeau, M.-L., Ollivier, B., Joulian, C., Baena, S., 2007. *Desulfomicrobium thermophilum* sp. nov., a novel thermophilic sulphate-reducing bacterium isolated from a terrestrial hot spring in Colombia. Extremophiles 11 (2), 295–303. https://doi.org/10.1007/s00792-006-0039-9.

Torres, C.I., Marcus, A.K., Rittmann, B.E., 2007. Kinetics of consumption of fermentation products by anode-respiring bacteria. Appl. Microbiol. Biotechnol. 77 (3), 689–697 Dec.

Venkata Mohan, S., Veer Raghavulu, S., Sarma, P.N., 2008. Influence of anodic biofilm growth on bioelectricity production in single chambered mediatorless microbial fuel cell using mixed anaerobic consortia. Biosens. Bioelectron. 24 (1), 41–47 Sep.

Vilas Boas, J., Oliveira, V.B., Marcon, L.R.C., Simões, M., Pinto, A.M.F.R., 2019. Optimization of a single chamber microbial fuel cell using *Lactobacillus pentosus*: Influence of design and operating parameters. Sci. Total Environ. 648, 263–270 Jan.

Vogel, E., 1980. Multipulse precession of spinning spacecraft with flexible appendages. Guidance and Control Conference https://doi.org/10.2514/6.1980-1782.

Watson, V.J., Logan, B.E., 2010. Power production in MFCs inoculated with *Shewanella oneidensis* MR-1 or mixed cultures. Biotechnology and Bioengineering 105 (3), 489–498. https://doi.org/10.1002/bit.22556.

Wei, L., Han, H., Shen, J., 2013. Effects of temperature and ferrous sulfate concentrations on the performance of microbial fuel cell. International Journal of Hydrogen Energy 38 (25), 11110–11116. https://doi.org/10.1016/j.ijhydene.2013.01.019.

Xing, D., Zuo, Y., Cheng, S., Regan, J.M., Logan, B.E., 2008. Electricity generation by *Rhodopseudomonas palustris* DX-1. Environ. Sci. Technol. 42 (11), 4146–4151 Jun.

Yang, W., Kim, K.-Y., Logan, B.E., 2015. Development of carbon free diffusion layer for activated carbon air cathode of microbial fuel cells. Bioresour. Technol. 197, 318–322. https://doi.org/10.1016/j.biortech.2015.08.119.

Yee, M.O., Snoeyenbos-West, O., Thamdrup, B., Ottosen, L. D. M., Rotaru, A.E., et al., 2019. Extracellular Electron Uptake by Two *Methanosarcina* Species.

Yong, Y.-C., Yu, Y.-Y., Li, C.-M., Zhong, J.-J., Song, H., 2011. Bioelectricity enhancement via overexpression of quorum sensing system in Pseudomonas aeruginosa-inoculated microbial fuel cells. Biosens. Bioelectron. 30 (1), 87–92 Dec.

Zhang, Y., Liu, F., Xu, H., Xiao, L., 2019. Extraction of electrons by magnetite and ferrihydrite from hydrogen-producing *Clostridium bifermentans* by strengthening the acetate production pathway. Science China Technological Sciences 62 (10), 1719–1725. https://doi.org/10.1007/s11431-018-9460-9.

Zheng, Y., Xiao, Y., Yang, Z.H., Wu, S., Xhu, H.J, Liang, F.Y., et al., 2014. The bacterial communities of bioelectrochemical systems associated with the sulfate removal under different pHs. Process Biochemistry 49 (8), 1345–1351. https://doi.org/10.1016/j.procbio.2014.04.019.